DEPARTAMENTO DE MATEMÁTICA APLICADA

Relatório Técnico

RT-MAP-0008

"A non-linear Galerkin method for the shallow-water equations on periodic domains"

Saulo R. M. Barros,
José W. Cárdenas

September, 2000

UNIVERSIDADE DE SÃO PAULO
INSTITUTO DE MATEMÁTICA E ESTATÍSTICA
SÃO PAULO — BRASIL

A non-linear Galerkin method for the shallow-water equations on periodic domains

Saulo R. M. Barros and José W. Cárdenas[1]

Departamento de Matemática Aplicada, Universidade de São Paulo, R. do Matão, 1010, 05508-900 São Paulo, Brazil and Laboratório Nacional de Computação Científica, Av. Getúlio Vargas, 333, 25651-070, Petrópolis, R.J., Brazil

E-mail: saulo@ime.usp.br; cardenas@lncc.br

A non-linear Galerkin method for the shalow-water equations is developed, based on spectral transforms. The scheme is compared to a pseudo-spectral Galerkin method. Our numerical results indicate that the non-linear scheme has the potential advantage of providing similar accuracy at a lower cost than the Galerkin method. The non-linear method has also less restrictive stability conditions.

1. INTRODUCTION

Non-linear Galerkin methods were first introduced by Marion and Temam [12] for Navier-Stokes equations, from a theoretical point of view. The technique relies on the theory of approximate inertial manifolds [8] (see also [2] for the shallow-water equations) and employs a decomposition of the solution into its small and large-scale components. Applications of the method have been developed, among others, for the Burgers equation [9, 4] and Navier-Stokes equations [10, 6, 3].

In this article we propose a non-linear Galerkin method for the shallow-water equations on two-dimensional domains with periodic boundary conditions (the equations are formulated as in the model proposed by Lorenz [11], on a f-plane). The shallow-water equations differ from the incompressible Navier-Stokes equations by the inclusion of the coriolis force and by a different mass-conservation equation. In particular, a shallow-water flow is not divergence-free and the equations can not be projected on the space of non-divergent velocities, as tipically done for the Navier-Stokes equations. In the scheme we propose, the velocity components and the geopotential height are expanded as double Fourier series, truncated at a certain resolution and the solution space is decomposed into low and high modes. Some non-linear interaction terms are neglected and, through projection of the equations onto the solution spaces, Galerkin equations for the low and high modes are derived. The implementation of the scheme is made efficient by the use of the spectral transform method [7, 13] to compute the projections. These are computed exactly, with

[1] Partially supported by the Brazilian Research Council (CNPq).

no aliasing, by choosing auxiliary grids of appropriate sizes. The time-discretization is based on a semi-implicit method, leading to CFL stability constraints guided by the flow velocities (and not by the high phase speeds of the gravity-wave modes of the shallow-water equations). The stability conditions are less restrictive than for the Galerkin method. These facts are shown in a linear stability analysis and verified in the numerical experiments.

A non-linear Galerkin method for the shallow-water equations has been proposed in [5]. There, two families of basis functions for the velocity field are employed, one composed by purely rotational and one by purely divergent fields (these basis functions have to be precomputed). Their approach also differs from ours in the time discretization (they employ predictor corrector schemes) and in the numerical treatment of the equations, since they don't use spectral transforms (which we feel to be fundamental for efficiency).

The appropriate truncation number for a non-linear Galerkin scheme depends on the spectral distribution of energy [3, 5]. In any case, if the high modes are resolved only up to a certain wave number, a corresponding Galerkin method using the same truncation should provide results at least as good, since it uses more information than the non-linear scheme (in which some non-linear interactions are neglected). The potential advantage of the non-linear Galerkin scheme is to provide essentially the same accuracy at a reduced computational cost. We compared the non-linear method with a corresponding Galerkin scheme and obtained numerical evidence of this advantage of the non-linear method. We feel the technique attractive for applications and we are investigating its use on global models on the sphere, aiming numerical weather prediction.

The paper is structured as follows. It begins with the description of the equations in section 2, followed by the presentation of the Galerkin method in section 3. Section 4 is dedicated to the non-linear Galerkin method and in section 5 we develop the linear stability analysis of the Galerkin schemes. Numerical results are presented in section 6 and the paper is closed with some conclusions.

2. THE SHALLOW-WATER EQUATIONS

We consider the shallow-water equations in adimensional form as proposed by Lorenz [11], on a two-dimensional rectangular domain (the so called f-plane), with periodic boundary conditions. Diffusion and a mass-forcing term are explicitly included. The equations are given by:

$$\begin{aligned} \frac{\partial u}{\partial t} + uu_x + vu_y - v + z_x - \nu_0 \Delta u &= 0 \\ \frac{\partial v}{\partial t} + uv_x + vv_y + u + z_y - \nu_0 \Delta v &= 0 \\ \frac{\partial z}{\partial t} + uz_x + vz_y + (g_0 + z)(u_x + v_y) - \kappa_0 \Delta z &= F, \end{aligned} \tag{1}$$

where the unknows are the two velocity components u and v and the geopotential height z; the domain is $\Omega = [0, 2\pi] \times [0, 2\pi]$. The terms $-v$ and u in the first two equations correspond to the adimensional form of the coriolis force, ν_0 and κ_0 are the diffusion coefficients and F is the (time independent) mass-forcing term.

The shallow-water equations are distinguished from the $2D$-incompressible Navier-Stokes equations by including effects of the earth rotation in the coriolis terms and by having a different mass continuity equation. In particular, the flow is not divergence-free and a Galerkin method for these equations can not employ a projection on the space of non divergent veloc-

ities. The shallow-water equations are often employed in models for ground-water, oceanic and atmospheric flows.

3. A PSEUDO-SPECTRAL GALERKIN METHOD FOR THE EQUATIONS

The shallow-water equations admit solutions evolving in different time scales. They present slower modes, the Rossby waves, and the much faster evolving gravity waves. While one is normally interested in following the large scale motion of the Rossby waves, the presence of the gravity waves, in spite of the fact that they usually carry little energy, poses severe stability restrictions for explicit schemes, due to their high phase speed. Therefore, it is important to adopt some degree of implicitness in the numerical schemes for these equations, in order to attenuate the CFL stability constraints.

We propose here a semi-implicit pseudo-spectral Galerkin method for system (1). The prognostic fields u, v and z will be expanded as double Fourier series,

$$\begin{bmatrix} u_N(x,y,t) \\ v_N(x,y,t) \\ z_N(x,y,t) \end{bmatrix} = \sum_{l,k \in I_N} \begin{bmatrix} \hat{u}_{lk}(t) \\ \hat{v}_{lk}(t) \\ \hat{z}_{lk}(t) \end{bmatrix} e^{i(lx+ky)}, \tag{2}$$

where

$$I_N = \left\{ (l,k) : -\frac{N}{2} + 1 \le l,k \le \frac{N}{2} \right\}. \tag{3}$$

The truncated expansion can be seen as the result of the projection P_N from the space H_{per} of functions given by double Fourier series onto $U_N = \text{span}\{e^{i(lx+ky)} : (l,k) \in I_N\}$. We first consider a second-order semi-implicit time discretization of (1), where the terms giving rise to the fast gravity waves (like the geopotential gradient) will be treated implicitly, while the non-linear terms will be discretized explicitly by a leap-frog type scheme. The complete time discretization is given by:

$$\begin{aligned} u^{n+1} - \Delta t\, v^{n+1} + \Delta t\, z_x^{n+1} - \nu_0\, \Delta t\, \Delta u^{n+1} &= r_{1a}^{n-1} + r_{1b}^n \\ v^{n+1} + \Delta t\, u^{n+1} + \Delta t\, z_y^{n+1} - \nu_0\, \Delta t\, \Delta v^{n+1} &= r_{2a}^{n-1} + r_{2b}^n \\ z^{n+1} + g_0 \Delta t\, (u_x^{n+1} + v_y^{n+1}) - \kappa_0\, \Delta t\, \Delta z^{n+1} &= r_{3a}^{n-1} + r_{3b}^n \end{aligned} \tag{4}$$

where a superscript n refers to the variables at time $t_n = n\Delta t$, and

$$\begin{aligned} r_{1a}^{n-1} &= u^{n-1} + \Delta t\, v^{n-1} - \Delta t\, z_x^{n-1} + \nu_0\, \Delta t\, \Delta u^{n-1} \\ r_{2a}^{n-1} &= v^{n-1} - \Delta t\, u^{n-1} - \Delta t\, z_y^{n-1} + \nu_0\, \Delta t\, \Delta v^{n-1} \\ r_{3a}^{n-1} &= z^{n-1} - \Delta t\, g_0 (u_x^{n-1} + v_y^{n-1}) + \kappa_0\, \Delta t\, \Delta z^{n-1} \end{aligned} \tag{5}$$

$$\begin{aligned} r_{1b}^n &= -2\Delta t\, (u^n u_x^n + v^n u_y^n) \\ r_{2b}^n &= -2\Delta t\, (u^n v_x^n + v^n v_y^n) \\ r_{3b}^n &= -2\Delta t\, ((z^n u^n)_x + (z^n v^n)_y + F)\ . \end{aligned} \tag{6}$$

The Galerkin scheme is obtained through the projection of the time discretizated equations on U_N:

$$
\begin{aligned}
u_N^{n+1} - \Delta t\, v_N^{n+1} + \Delta t\, z_{N,x}^{n+1} - \nu_0\, \Delta t\, \Delta u_N^{n+1} &= P_N(r_{1a}^{n-1} + r_{1b}^{n}) \\
v_N^{n+1} + \Delta t\, u_N^{n+1} + \Delta t\, z_{N,y}^{n+1} - \nu_0\, \Delta t\, \Delta v_N^{n+1} &= P_N(r_{2a}^{n-1} + r_{2b}^{n}) \\
z_N^{n+1} + g_0 \Delta t\, (u_{N,x}^{n+1} + v_{N,y}^{n+1}) - \kappa_0\, \Delta t\, \Delta z_N^{n+1} &= P_N(r_{3a}^{n-1} + r_{3b}^{n}).
\end{aligned} \tag{7}
$$

Assuming for the moment that the projections in the right-hand-side of (7) have been computed, this linear system can be decomposed for each spectral component $(l,k) \in I_N$ as:

$$
\begin{bmatrix}
1+\nu_0\,\gamma_{lk} & -\Delta t & \mathrm{i}\, l\, \Delta t \\
\Delta t & 1+\nu_0\,\gamma_{lk} & \mathrm{i}\, k\, \Delta t \\
\mathrm{i}\, l\, g_0 \Delta t & \mathrm{i}\, k\, g_0 \Delta t & 1+\kappa_0\,\gamma_{lk}
\end{bmatrix}
\cdot
\begin{bmatrix} \hat{u}_{lk}^{n+1} \\ \hat{v}_{lk}^{n+1} \\ \hat{z}_{lk}^{n+1} \end{bmatrix}
=
\begin{bmatrix} \hat{r}_{1a,lk}^{n-1} + \hat{r}_{1b,lk}^{n} \\ \hat{r}_{2a,lk}^{n-1} + \hat{r}_{2b,lk}^{n} \\ \hat{r}_{3a,lk}^{n-1} + \hat{r}_{3b,lk}^{n} \end{bmatrix} \tag{8}
$$

where $\gamma_{lk} = \Delta t \lambda_{lk}$ and $\lambda_{lk} = l^2 + k^2$ is the corresponding eigenvalue of minus the Laplacian.
System (8) is written as a system for $(\hat{u}_{lk}^{n+1}, \hat{v}_{lk}^{n+1})$ (depending on the $\hat{z}_{lk}^{n+1}$ variable)

$$
\begin{bmatrix}
(1+\nu_0\,\gamma_{lk}) & -\Delta t \\
\Delta t & (1+\nu_0\,\gamma_{lk})
\end{bmatrix}
\cdot
\begin{bmatrix} \hat{u}_{lk}^{n+1} \\ \hat{v}_{lk}^{n+1} \end{bmatrix}
=
\begin{bmatrix} \hat{r}_{1a,lk}^{n-1} + \hat{r}_{1b,lk}^{n} - \mathrm{i}\, l\, \Delta t\, \hat{z}_{lk}^{n+1} \\ \hat{r}_{2a,lk}^{n-1} + \hat{r}_{2b,lk}^{n} - \mathrm{i}\, k\, \Delta t\, \hat{z}_{lk}^{n+1} \end{bmatrix}
$$

whose solution is given by

$$
\begin{bmatrix} \hat{u}_{lk}^{n+1} \\ \hat{v}_{lk}^{n+1} \end{bmatrix}
= \frac{1}{\theta_{lk}}
\begin{bmatrix} \hat{s}_{1,lk} - \mathrm{i}\,(l\,\Delta t\,(1+\nu_0\,\gamma_{lk}) + k\,\Delta^2 t)\,\hat{z}_{lk}^{n+1} \\ \hat{s}_{2,lk} + \mathrm{i}\,(l\,\Delta^2 t - k\,\Delta t\,(1+\nu_0\,\gamma_{lk}))\,\hat{z}_{lk}^{n+1} \end{bmatrix}, \tag{9}
$$

where

$$
\begin{aligned}
\mathrm{i} &= \sqrt{-1} \\
\theta_{lk} &= (1+\nu_0\,\gamma_{lk})^2 + \Delta^2 t \\
\hat{s}_{1,lk} &= (1+\nu_0\,\gamma_{lk})\,(\hat{r}_{1a,lk}^{n-1} + \hat{r}_{1b,lk}^{n}) + \Delta t\,(\hat{r}_{2a,lk}^{n-1} + \hat{r}_{2b,lk}^{n}) \\
\hat{s}_{2,lk} &= -\Delta t\,(\hat{r}_{1a,lk}^{n-1} + \hat{r}_{1b,lk}^{n}) + (1+\nu_0\,\gamma_{lk})\,(\hat{r}_{2a,lk}^{n-1} + \hat{r}_{2b,lk}^{n})\ .
\end{aligned} \tag{10}
$$

The combination of the two equations in (9) (equivalent to building the divergence of the new velocity field) provides the expression

$$
\mathrm{i}\,(l\,\hat{u}_{lk}^{n+1} + k\,\hat{v}_{lk}^{n+1}) = \frac{\left(\mathrm{i}\,(l\,\hat{s}_{1,lk} + k\,\hat{s}_{2,lk}) + \Delta t\,(1+\nu_0\,\gamma_{lk})\lambda_{lk}\,\hat{z}_{lk}^{n+1}\right)}{\theta_{lk}}, \tag{11}
$$

which when employed in the third equation of (8) leads to

$$
\hat{z}_{lk}^{n+1} = \frac{1}{\alpha_{lk}}\left(\hat{r}_{3a,lk}^{n-1} + \hat{r}_{3b,lk}^{n} - \mathrm{i}\,\frac{g_0\,\Delta t}{\theta_{lk}}(l\,\hat{s}_{1,lk} + k\,\hat{s}_{2,lk})\right) \tag{12}
$$

with

$$
\alpha_{lk} = 1 + \frac{g_0\,\Delta t\,\gamma_{lk}}{\theta_{lk}}(1+\nu_0\,\gamma_{lk}) + \kappa_0\,\gamma_{lk}. \tag{13}
$$

Altogether, we solve (8) by first deriving the value of $\hat{z}_{lk}^{n+1}$ from (12) and then using it in (9).

For the solution of (7) it remains to explain how to compute the projections of the right hand side. Since they involve the non-linear terms (including products of the variables), they can not be computed directly from the spectral coefficients in a efficient way. Instead, we employ the so called spectral transform method [7, 13], using an auxiliary grid

$$J_N = \left\{(x_r, y_s): \ x_r = \frac{2\pi(r-1)}{N}, \ y_s = \frac{2\pi(s-1)}{N}, \quad r,s = 1,\cdots,N\right\}, \quad (14)$$

where we can evaluate the function and derivative values involved in the right hand side of (7) (through Fourier transforms). On the grid, the products can be trivially formed and added. In order to project the right hand side of (7) onto U_N a Fourier transform of the grid values is employed, leading to the spectral coeffcients. However, the product of two functions in U_N (like u and u_x) lies in U_{2N}, and if it is evaluated on the grid J_N and transformed back to get the spectral representation, the high modes ($N+1$ to $2N$) will be aliased with the lower modes. This spurious transfer of energy from high to low modes is a potential source of (non-linear) instability in the scheme. If we use the grid J_{2N} instead, we get the correct coefficients of the product term in U_{2N} and therefore the correct projection onto U_N. But for this purpose, it is sufficient to employ grid $J_{3N/2}$ where aliasing occur only in the frequency range from $N+1$ to $3N/2$ and an alias free projection onto U_N will be computed (see [1]). This is the smallest grid to guarantee an alias free computation and will be chosen in efficient computations. In summary, a complete time-step will consist of the computation of the right hand side of (7) on grid $J_{3N/2}$ amounting to Fourier transforms of u, v, z and their gradients, in a total of 9 fields transformed. The products are then computed on the grid and the right hand sides of (7) are transformed back. The system can then be solved and the time-step completed. The computational costs are dominated by the 12 transforms per time-step, on a grid of size $3N/2 \times 3N/2$. Therefore, the computational costs will be of the order $\vartheta(27N^2 \log_2(3N/2))$

4. THE NON-LINEAR GALERKIN METHOD

In non-linear Galerkin methods the solution space (H_{per} in this case) is decomposed on two subspaces: a space of low modes and its complement (see [12]). From a pratical point of view, it is necessary to take the complement (space of high modes) also as a finite-dimensional space. We will adopt the following splitting of $U_N = U_{N/2} + W_N$ with corresponding projections $P_{N/2}: H_{per} \to U_{N/2}$, $Q_N: H_{per} \to W_N$ (and $P_N - P_{N/2} = Q_N$), leading to a decomposition of the velocity and geopotential fields:

$$\begin{aligned} u_N &= p_1 + q_1, \qquad (p_1 = P_{N/2}(u), \ q_1 = Q_N(u)) \\ v_N &= p_2 + q_2, \qquad (p_2 = P_{N/2}(v), \ q_2 = Q_N(v)) \\ z_N &= p_3 + q_3, \qquad (p_3 = P_{N/2}(z), \ q_3 = Q_N(z)) \\ F_N &= F_1 + F_2, \qquad (F_1 = P_{N/2}F, \ F_2 = Q_N F). \end{aligned} \quad (15)$$

Projecting the shallow-water equations onto the low ($U_{N/2}$) and high (W_N) modes spaces, we obtain the corresponding systems:

$$\begin{aligned}
\frac{\partial p_1}{\partial t} - p_2 + \frac{\partial p_3}{\partial x} - \nu_0 \Delta p_1 &= s_1 \\
\frac{\partial p_2}{\partial t} + p_1 + \frac{\partial p_3}{\partial y} - \nu_0 \Delta p_2 &= s_2 \\
\frac{\partial p_3}{\partial t} + g_0 \left(\frac{\partial p_1}{\partial x} + \frac{\partial p_2}{\partial x} \right) - \kappa_0 \Delta p_3 &= s_3
\end{aligned} \tag{16}$$

$$\begin{aligned}
\frac{\partial q_1}{\partial t} - q_2 + \frac{\partial q_3}{\partial x} - \nu_0 \Delta q_1 &= s_4 \\
\frac{\partial q_2}{\partial t} + q_1 + \frac{\partial q_3}{\partial y} - \nu_0 \Delta q_2 &= s_5 \\
\frac{\partial q_3}{\partial t} + g_0 \left(\frac{\partial q_1}{\partial x} + \frac{\partial q_2}{\partial x} \right) - \kappa_0 \Delta q_3 &= s_6
\end{aligned} \tag{17}$$

The equations (16) constitute the system for the low modes and the equations (17), the system for the high modes. The non-linear interaction terms (s_1 to s_6) from the low and high mode systems are given by:

$$\begin{aligned}
s_1 &= P_{N/2} \, (-(p_1 + q_1)(p_1 + q_1)_x - (p_2 + q_2)(p_1 + q_1)_y \,) \\
s_2 &= P_{N/2} \, (-(p_1 + q_1)(p_2 + q_2)_x - (p_2 + q_2)(p_2 + q_2)_y \,) \\
s_3 &= P_{N/2} \, (F - [(p_3 + q_3)(p_1 + q_1)]_x - [(p_3 + q_3)(p_2 + q_2)]_y \,) \\
s_4 &= Q_N \, (-(p_1 + q_1)(p_1 + q_1)_x - (p_2 + q_2)(p_1 + q_1)_y \,) \\
s_5 &= Q_N \, (-(p_1 + q_1)(p_2 + q_2)_x - (p_2 + q_2)(p_2 + q_2)_y \,) \\
s_6 &= Q_N \, (F - [(p_3 + q_3)(p_1 + q_1)]_x - [(p_3 + q_3)(p_2 + q_2)]_y \,) .
\end{aligned} \tag{18}$$

The systems (16) and (17) are equivalent to the Galerkin discretization on U_N, described in the last section. For the definition of the non-linear Galerkin method we will now neglect the interaction between higher modes in the equation for the low modes. In the equation for the high modes we also discard the interaction between low and high modes, and allow for the possibility of considering it as a diagnostic equation, droping the temporal derivates. The expressions for s_1 to s_6 in the non-linear Galerkin method will then be simplified as:

$$\begin{aligned}
s_1 &= P_{N/2} \, (-p_1 \, (p_1 + q_1)_x - q_1 \, p_{1,x} - p_2 \, (p_1 + q_1)_y - q_2 \, p_{1,y} \,) \\
s_2 &= P_{N/2} \, (-p_1 \, (p_2 + q_2)_x - q_1 \, p_{2,x} - p_2 \, (p_2 + q_2)_y - q_2 \, p_{2,y} \,) \\
s_3 &= P_{N/2} \, (\, F - (p_3(p_1 + q_1))_x - (q_3 \, p_1)_x - (p_3(p_2 + q_2))_y - (q_3 \, p_2)_y \,) \\
s_4 &= Q_N \, (\, -p_1 \, p_{1,x} - p_2 \, p_{1,y} \,) \\
s_5 &= Q_N \, (\, -p_1 \, p_{2,x} - p_2 \, p_{2,y} \,) \\
s_6 &= Q_N \, (\, F - (p_3 \, p_1)_x - (p_3 \, p_2)_y \,) .
\end{aligned} \tag{19}$$

These simplifications are motivated by the theory of Approximate Inertial Manifolds in which the small wave lengths (high modes) are approximately determined by the large ones (low modes), through the inertial manifolds [8, 2] (which are approximated here by the diagnostic equation for the high modes).

The numerical discretization of the non-linear Galerkin method will follow the same lines of our Galerkin scheme. We employ a semi-implicit temporal discretization on a

pseudo-spectral method, applying spectral transforms to compute non-linear products. The projections on the high and low modes spaces will be computed exactly in an alias free scheme.

Considering the equation for the high modes as a diagnostic equation, we have:

$$\begin{aligned} p_1^{n+1} - \Delta t\, p_2^{n+1} + \Delta t\, p_{3,x}^{n+1} - \nu_0\, \Delta t\, \Delta p_1^{n+1} &= S_1^{n-1} + 2\Delta t\, s_1^{n,n+1} \\ p_2^{n+1} + \Delta t\, p_1^{n+1} + \Delta t\, p_{3,y}^{n+1} - \nu_0\, \Delta t\, \Delta p_2^{n+1} &= S_2^{n-1} + 2\Delta t\, s_2^{n,n+1} \\ p_3^{n+1} + g_0 \Delta t\, (p_{1x}^{n+1} + p_{2y}^{n+1}) - \kappa_0\, \Delta t\, \Delta p_3^{n+1} &= S_3^{n-1} + 2\Delta t\, s_3^{n,n+1} \end{aligned} \tag{20}$$

$$\begin{aligned} -q_2^{n+1} + q_{3,x}^{n+1} - \nu_0\, \Delta q_1^{n+1} = s_4^n &= Q_N\ (\, -p_1^n\, p_{1,x}^n - p_2^n\, p_{1,y}^n\,) \\ q_1^{n+1} + q_{3,y}^{n+1} - \nu_0\, \Delta q_2^{n+1} = s_5^n &= Q_N\ (\, -p_1^n\, p_{2,x}^n - p_2^n\, p_{2,y}^n\,) \\ g_0\, (q_{1x}^{n+1} + q_{2y}^{n+1}) - \kappa_0\, \Delta q_3^{n+1} = s_6^n &= Q_N\ (\, F - (p_3^n\, p_1^n)_x - (p_3^n\, p_2^n)_y\,)\ , \end{aligned} \tag{21}$$

with superscripts refering to time instants. The linear terms at time t_{n-1} in the equation for low modes are given by:

$$\begin{aligned} S_1^{n-1} &= p_1^{n-1} + \Delta t\, p_2^{n-1} - \Delta t\, p_{3x}^{n-1} + \nu_0\, \Delta t\, \Delta p_1^{n-1} \\ S_2^{n-1} &= p_2^{n-1} - \Delta t\, p_1^{n-1} - \Delta t\, p_{3y}^{n-1} + \nu_0\, \Delta t\, \Delta p_2^{n-1} \\ S_3^{n-1} &= p_3^{n-1} - \Delta t\, g_0 (p_{1x}^{n-1} + p_{2y}^{n-1}) + \kappa_0\, \Delta t\, \Delta p_3^{n-1}. \end{aligned} \tag{22}$$

The non-linear terms are discretized as follows:

$$\begin{aligned} s_1^{n,n+1} &= P_{N/2}\ (-p_1^n\, (p_1^n + q_1^{n+1})_x - q_1^{n+1}\, p_{1,x}^n - p_2^n\, (p_1^n + q_1^{n+1})_y - q_2^{n+1}\, p_{1,y}^n\,) \\ s_2^{n,n+1} &= P_{N/2}\ (-p_1^n\, (p_2^n + q_2^{n+1})_x - q_1^{n+1}\, p_{2,x}^n - p_2^n\, (p_2^n + q_2^{n+1})_y - q_2^{n+1}\, p_{2,y}^n\,) \\ s_3^{n,n+1} &= P_{N/2}\ (\, F - (p_3^n (p_1^n + q_1^{n+1}))_x - (q_3^{n+1}\, p_1^n)_x - (p_3^n (p_2^n + q_2^{n+1}))_y - \\ &\qquad -(q_3^{n+1}\, p_2^n)_y\,) \end{aligned} \tag{23}$$

The equations are transformed into equations for the spectral coefficients of low modes ($(l,k) \in U_{N/2}$):

$$\begin{bmatrix} 1+\nu_0\,\gamma_{lk} & -\Delta t & \mathrm{i}\,l\,\Delta t \\ \Delta t & 1+\nu_0\,\gamma_{lk} & \mathrm{i}\,k\,\Delta t \\ \mathrm{i}\,l\,g_0\Delta t & \mathrm{i}\,k\,g_0\Delta t & 1+\kappa_0\,\gamma_{lk} \end{bmatrix} \cdot \begin{bmatrix} \hat{p}_{1,lk}^{n+1} \\ \hat{p}_{2,lk}^{n+1} \\ \hat{p}_{3,lk}^{n+1} \end{bmatrix} = \begin{bmatrix} \hat{S}_{1,lk}^{n-1} + 2\Delta t\, \hat{s}_{1,lk}^{n,n+1} \\ \hat{S}_{2,lk}^{n-1} + 2\Delta t\, \hat{s}_{2,lk}^{n,n+1} \\ \hat{S}_{3,lk}^{n-1} + 2\Delta t\, \hat{s}_{3,lk}^{n,n+1} \end{bmatrix} \tag{24}$$

and for the high modes ($(l,k) \in W_N$):

$$\begin{bmatrix} \nu_0\,\lambda_{lk} & -1 & \mathrm{i}\,l \\ 1 & \nu_0\,\lambda_{lk} & \mathrm{i}\,k \\ \mathrm{i}\,l\,g_0 & \mathrm{i}\,k\,g_0 & \kappa_0\,\lambda_{lk} \end{bmatrix} \cdot \begin{bmatrix} \hat{q}_{1,lk}^{n+1} \\ \hat{q}_{2,lk}^{n+1} \\ \hat{q}_{3,lk}^{n+1} \end{bmatrix} = \begin{bmatrix} \hat{s}_{4,lk}^{n} \\ \hat{s}_{5,lk}^{n} \\ \hat{s}_{6,lk}^{n} \end{bmatrix}. \tag{25}$$

Assuming the right hand side of (25) to be known, it can be solved as system (8) leading to the new values of $\hat{q}_1$, $\hat{q}_2$ and $\hat{q}_3$. These high modes are used in the right hand side of (24), which can then be solved as (8) for each $(l,k) \in U_{N/2}$. The evaluation of the right hand side of the systems for the low and high modes involves non-linear terms. For this purpose

we employ spectral transforms, choosing appropriate auxiliary grids to garantee alias free results and an efficient scheme.
We need to compute products of low modes with either low or high modes, and then project the results onto $U_{N/2}$ or W_N. For functions ϕ, θ in $U_{N/2}$ the product $\phi\theta$ lies in U_N. With an $N \times N$ grid a two dimensional FFT will provide the correct values of all spectral coefficients of $\phi\theta$ and therefore the two projections $P_{N/2}(\phi\theta)$ and $Q_N(\phi\theta)$are obtained alias free. For ϕ in $U_{N/2}$ and θ in W_N the product lies in $U_{3N/2}$. With an $N \times N$ grid only the modes with wave number up to $N/2$ will be obtained alias free. But that's all we need to have $P_{N/2}(\phi\theta)$ computed correctly. Therefore an $N \times N$ grid will be suficient for obtaining all the right hand sides with no aliasing.

In summary, a time-step of the method will proceed as follows, assuming $\hat{p}^{n-1}_{1,lk}$, $\hat{p}^{n-1}_{2,lk}$, $\hat{p}^{n-1}_{3,lk}$ for $(l,k) \in I_{N/2}$ and the values of p^n_1, p^n_{1x}, p^n_{1y}, p^n_2, p^n_{2x}, p^n_{2y}, p^n_3, p^n_{3x}, p^n_{3y}, on a $N \times N$ grid to be known.

a) Computation of high modes at t_{n+1}:

a1) Compute s^n_4, s^n_5, s^n_6 on the grid and apply Fourier transforms to get $\hat{s}^n_{4,lk}$, $\hat{s}^n_{5,lk}$, $\hat{s}^n_{6,lk}$ for $(l,k) \in I_N$.

a2) Solve for $\hat{q}^{n+1}_i$ $(i = 1, \cdots 3) \in W_N$.

a3) Compute the values of q^{n+1}_i, $\partial_x q^{n+1}_i, \partial_y q^{n+1}_i$, $(i = 1, \cdots 3)$ on the $N \times N$ grid, for $q^{n+1}_i \in W_N$.

b) Computation of the low modes at t_{n+1}:

b1) Using the values computed in step *a3)* evaluate $s^{n,n+1}_i$, $i = 1, 2, 3$ on the $N \times N$ grid and use FFT's to get he corresponding spectral coefficients of their projection onto $U_{N/2}$.

b2) Complete the right hand side with the linear terms S^{n-1}_i, $i = 1, 2, 3$ and solve the equations for $\hat{p}^{n+1}_i$ in $U_{N/2}$.

b3) Generate the values of p^{n+1}_i, $\partial_x p^{n+1}_i$, $\partial_y p^{n+1}_i$, $(i = 1, \cdots 3)$ on the $N \times N$ grid, which shall be used in the following time-step.

Altogether, 24 two-dimensional FFT's on $N \times N$ grids will be carried out, 12 when computing the high modes and 12 for the low modes. The total computational work will be of the order of $\vartheta(24N^2 \log_2(3N^2/2)$. This work compares favorably to the $\vartheta(27N^2 \log_2(3N^2/2)$ of the linear Galerkin method (on U_N), which needed a $3N/2 \times 3N/2$ grid for alias free results.

We also consider the possibility of freezing the high modes coefficients for several time-steps. In this case the total computational cost consists essentially of the costs for the low modes equation, being reduced almost by a factor of two.

5. LINEAR STABILITY ANALYSIS

We present a linear stability analysis for the pseudo-spectral linear Galerkin method described in section (2). The discrete equations are given by:

$$\frac{\vec{V}_N^{n+1}-\vec{V}_N^{n-1}}{2\,\Delta t}+P_N((\vec{V}_N^n\cdot\nabla)\vec{V}_N^n)+\vec{k}\times\frac{\vec{V}_N^{n+1}+\vec{V}_N^{n-1}}{2}+$$
$$+\nabla\left(\frac{z_N^{n+1}+z_N^{n-1}}{2}\right)-\nu_0\,\Delta\left(\frac{\vec{V}_N^{n+1}+\vec{V}_N^{n-1}}{2}\right)=0 \qquad (26)$$
$$\frac{z_N^{n+1}-z_N^{n-1}}{2\,\Delta t}+g_0\,\nabla\cdot\left(\frac{\vec{V}_N^{n+1}+\vec{V}_N^{n-1}}{2}\right)+P_N(\nabla\cdot(z_N^n\,\vec{V}_N^n))-$$
$$-\nu_0\,\Delta\left(\frac{z_N^{n+1}+z_N^{n-1}}{2}\right)=F_N,$$

with $\vec{V}_N=(u_N,v_N)\in U_N\times U_N$ and $z_N\in U_N$.

Linearizing system (26) around a state with constant velocity $\vec{U}$ leads to:

$$\frac{\vec{V}_N^{n+1}-\vec{V}_N^{n-1}}{2\,\Delta t}+(\,(\vec{U}\cdot\nabla)\vec{V}_N^n\,)+\vec{k}\times\frac{\vec{V}_N^{n+1}+\vec{V}_N^{n-1}}{2}+$$
$$+\nabla\left(\frac{z_N^{n+1}+z_N^{n-1}}{2}\right)-\nu_0\,\Delta\left(\frac{\vec{V}_N^{n+1}+\vec{V}_N^{n-1}}{2}\right)=0 \qquad (27)$$
$$\frac{z_N^{n+1}-z_N^{n-1}}{2\,\Delta t}+g_0\,\nabla\cdot\left(\frac{\vec{V}_N^{n+1}+\vec{V}_N^{n-1}}{2}\right)+\vec{U}\cdot\nabla z_N^n-$$
$$-\nu_0\,\Delta\left(\frac{z_N^{n+1}+z_N^{n-1}}{2}\right)=F_N.$$

We bild the scalar product of the first equation in (27) with $g_0(\vec{V}_N^{n+1}+\vec{V}_N^{n-1})$ and add it to the scalar product of the second equation with $(z_N^{n+1}+z_N^{n-1})$. This, after simplifying the terms originating from the geopotential and of the divergence, in presence of the periodic boundary conditions, leads to the expression:

$$g_0|\vec{V}_N^{n+1}|^2+|z_N^{n+1}|^2+g_0\nu_0\Delta t\|\vec{V}_N^{n+1}+\vec{V}_N^{n-1}\|^2+\nu_0\Delta t\|z_N^{n+1}+z_N^{n-1}\|^2$$
$$=g_0|\vec{V}_N^{n-1}|^2+|z_N^{n-1}|^2-2g_0\Delta t<\vec{U}\cdot\nabla\vec{V}_N^n,\vec{V}_N^{n+1}+\vec{V}_N^{n-1}>$$
$$-2\Delta t<\vec{U}\cdot\nabla z_N^n,z_N^{n+1}+z_N^{n-1}>+2\Delta t\;<F_N,z_N^{n+1}+z_N^{n-1}>,$$

where we have $\vec{V}=(u,v)$, $<u,v>=\int_\Omega uv$, $|\vec{V}|^2=|u|^2+|v|^2$, $|u|^2=<u,u>$, $\|\vec{V}\|^2=\|u\|^2+\|v\|^2$, $\|\vec{u}\|^2=|u_x|^2+|u_y|^2$.

We add $g_0|\vec{V}_N^n|^2+|z_N^n|^2$ to both sides of last equation, in order to get

$$G^{n+1}+g_0\nu_0\Delta t\|\vec{V}_N^{n+1}+\vec{V}_N^{n-1}\|^2+\nu_0\Delta t\|z_N^{n+1}+z_N^{n-1}\|^2=G^n+NLT+$$
$$+2\Delta t\;<F_N,z_N^{n+1}+z_N^{n-1}> \qquad (28)$$

where,

$$G^n = g_0|\vec{V}_N^n|^2 + g_0|\vec{V}_N^{n-1}|^2 + |z_N^n|^2 + |z_N^{n-1}|^2, \tag{29}$$

$$NLT = -2g_0\Delta t < \vec{U}\cdot\nabla\vec{V}_N^n, \vec{V}_N^{n+1} + \vec{V}_N^{n-1} > \\ -2\Delta t < \vec{U}\cdot\nabla z_N^n, z_N^{n+1} + z_N^{n-1} > . \tag{30}$$

For estimating the term with the mass forcing, we first observe that the integration of (27) on the whole domain leads to $\int_\Omega z_N^{n+1} - z_N^{n-1} = 2\Delta t \int_\Omega F_N$. This provides a limitation of the constant part of the solution (lets denote it by $\bar{z}_N^n$) of the type:

$$|\bar{z}_N^n| \leq Cn\Delta t|F_N| \ .$$

We now split $z_N^n = \bar{z}_N^n + \tilde{z}_N^n$, where $\tilde{z}_N^n$ has zero mean value. We then have:

$$\begin{aligned} 2\Delta t \ < F_N, z_N^{n+1} + z_N^{n-1} > \ &= \ 2\Delta t(< F_N, \bar{z}_N^{n+1} + \bar{z}_N^{n-1} > + < F_N, \tilde{z}_N^{n+1} + \tilde{z}_N^{n-1} >) \\ &\leq \ 2\Delta t \ |F_N| \ (|\bar{z}_N^{n+1} + \bar{z}_N^{n-1}| + |\tilde{z}_N^{n+1} + \tilde{z}_N^{n-1}|) \\ &\leq \ 2\Delta t \ |F_N| \ (2cn\Delta t|F_N| + c_1\|z_N^{n+1} + z_N^{n-1}\|) \qquad (31) \\ &\leq \ \frac{1}{2}\nu_0\Delta t \ \|z_N^{n+1} + z_N^{n-1}\|^2 + 2\Delta t(\frac{c_1^2}{\nu_0} + 2cn\Delta t) \ |F_N|^2 \ . \end{aligned}$$

In the last estimates we have used a Poincaré inequality and the algebraic inequality ($ab \leq a^2/4 + b^2$). We also observe, using the periodic boundary conditions, that:

$$-2g_0\Delta t < \vec{U}\cdot\nabla\vec{V}_N^n, \vec{V}_N^{n-1} > \ = \ 2g_0\Delta t < \vec{U}\cdot\nabla\vec{V}_N^{n-1}, \vec{V}_N^n >$$

Similarly $-2\Delta t < \vec{U}\cdot\nabla z_N^n, z_N^{n-1} >= 2\Delta t < \vec{U}\cdot\nabla z_N^{n-1}, z_N^n >$. Substituting in (30) we have:

$$\begin{aligned} NLT \ = \ &-2g_0\Delta t < \vec{U}\cdot\nabla\vec{V}_N^n, \vec{V}_N^{n+1} > -2\Delta t < \vec{U}\cdot\nabla z_N^n, z_N^{n+1} > + \\ &+2g_0\Delta t < \vec{U}\cdot\nabla\vec{V}_N^{n-1}, \vec{V}_N^n > +2\Delta t < \vec{U}\cdot\nabla z_N^{n-1}, z_N^n > = \ H^{n+1} - H^n, \end{aligned}$$

with

$$H^n \ = \ -2g_0\Delta t < \vec{U}\cdot\nabla\vec{V}_N^{n-1}, \vec{V}_N^n > -2\Delta t < \vec{U}\cdot\nabla z_N^{n-1}, z_N^n > .$$

Using the last expressions in (28) we obtain

$$\begin{aligned} G^{j+1} &\leq G^{j+1} + g_0\nu_0\Delta t\|\vec{V}_N^{j+1} + \vec{V}_N^{j-1}\|^2 + \frac{1}{2}\nu_0\Delta t\|z_N^{j+1} + z_N^{j-1}\|^2 \\ &\leq G^j + H^{j+1} - H^j + 2\Delta t(\frac{c_1^2}{\nu_0} + 2cn\Delta t) \ |F_N|^2. \qquad (32) \end{aligned}$$

Adding up for j from 1 to n results in

$$G^{n+1} \ \leq \ G^1 + H^{n+1} - H^1 + 2(\frac{c_1^2}{\nu_0} + 2cn\Delta t)n \ \Delta t \ |F_N|^2. \tag{33}$$

We can now limit:

$$\begin{aligned}|H^j| &\leq 2g_0\Delta t|\vec{U}|_\infty\|\vec{V}_N^{j-1}\|\,|\vec{V}_N^j| + 2\Delta t|\vec{U}|_\infty\|x_N^{j-1}\|\,|x_N^j| \\ &\leq 2g_0\sqrt{2}N\Delta t|\vec{U}|_\infty|\vec{V}_N^{j-1}|\,|\vec{V}_N^j| + 2\sqrt{2}N\Delta t|\vec{U}|_\infty|x_N^{j-1}|\,|x_N^j| \\ &\leq \sqrt{2}N\Delta t|\vec{U}|_\infty\left(g_0|\vec{V}_N^{j-1}|^2 + g_0|\vec{V}_N^j|^2 + |x_N^{j-1}|^2 + |x_N^j|^2\right) \\ &\leq (\sqrt{2}N\Delta t|\vec{U}|_\infty)\,G^j.\end{aligned}$$

It then follows from (33) that for any $T > 0$ fixed and $n\Delta t \leq T$:

$$(1 - \sqrt{2}N\Delta t\,|\vec{U}|_\infty)\,G^{n+1} \leq (1 + \sqrt{2}N\Delta t\,|\vec{U}|_\infty)\,G^1 + 2(\frac{c_1^2}{\nu_0} + 2cT)T\,|F_N|^2.$$

So, if $\Delta t < \frac{1}{\sqrt{2}N\,|\vec{U}|_\infty}$ we have

$$G^{n+1} \leq \frac{1 + \sqrt{2}N\Delta t\,|\vec{U}|_\infty}{1 - \sqrt{2}N\Delta t\,|\vec{U}|_\infty}\,G^1 + \frac{2(\nu_0^{-1}c_1^2 + 2cT)T}{1 - \sqrt{2}N\Delta t|\vec{U}|_\infty}\,|F_N|^2. \qquad (34)$$

We have therefore proved:

Proposition.- If Δt obeys the CFL condition $\Delta t < \frac{1}{\sqrt{2}N\,|\vec{U}|_\infty}$, then $G^n \leq c_2G^1 + c_3T\,|F_N|^2$, where c_2 and c_3 are constants, T a fixed time, and G^n is given by (29). It follows that the scheme is linearly stable.

Observation:
The same proof above applies for the non-linear galerkin method (with projections $P_{N/2}$ and Q_N). It will lead to the stability condition $\Delta t < \frac{1}{\sqrt{2}\frac{N}{2}\,|\vec{U}|_\infty}$, indicating that the CFL condition for the non-linear galerkin method is given by the equation for the low modes. This agrees with the fact that the equation for the high modes is employed as a diagnostic equation.
A analysis in which the linearization is done around a spatially variable basic state and the interaction between low and high modes is present in the resulting system is presented in [2].

6. NUMERICAL RESULTS

We present in this section numerical results obtained with the non-linear Galerkin method, which are compared with results from the pseudo-spectral Galerkin method described in section (4).

We first consider a smooth solution departing from a balanced (nearly stationary) initial state (dependent only on y) for $F = cos(y)/100$, given by

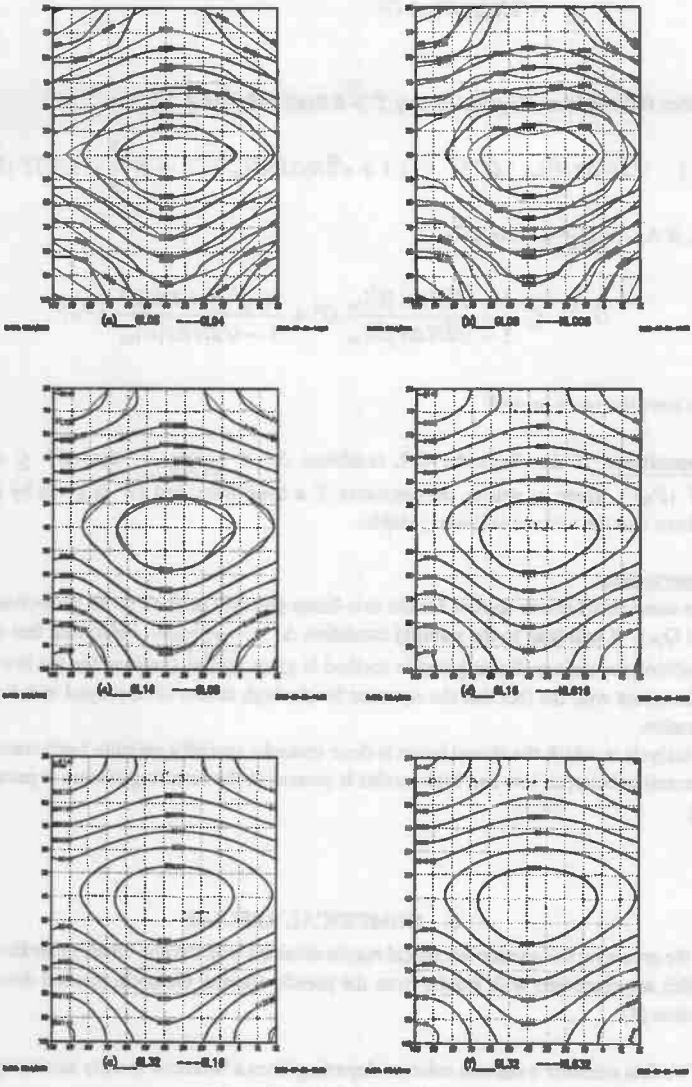

FIG. 1. Display of the geopotential field after 200 time-steps for several resolutions. In the left (plots a, c and e) we compare the results of the (linear) Galerkin method with truncations $N = 8, 16$ and 32 to the results of the same method at half resolution ($N = 4, 8$ and 16) respectively. In the right (plots b,d and f) the Galerkin (GL) method (with truncations $N = 8, 16$ and 32) is compared to the non-linear method (NLG) at same resolution (truncations $N = 8, 16$ and 32, respectively).

$$
\begin{aligned}
u &= \frac{1}{100\,\nu_0\,g_0}\,\mathrm{sen}(y) \\
v &= \frac{1}{100\,g_0}\,\mathrm{sen}(y) \\
z &= \frac{1}{100\,\nu_0\,g_0}\,\cos(y).
\end{aligned}
\tag{35}
$$

We adopt here a typical lenght $L = 1080Km$, height $h = 8km$, $g = 10m/s^2$, $f^{-1} = 10800s$ (f is the coriolis factor) and $\nu = \kappa = 2.25 \times 10^6 m^2/s$, which correspond to the choice $g_0 = 8, \nu_0 = \kappa_0 = 1/48$ in the adimensional model. We integrate the equations with a forcing term of the order of $F = \frac{L^2}{gf^3}$.

We first compared the different options for the non-linear method, using the equation for the high modes in diagnostic or prognostic form and either ativated every time-step or only every many steps. We concluded in favor of using the equations in diagnostic form (the results produced with the prognostic form were very similar) with the high modes frozen for many time-steps. The high modes can be kept frozen for many steps (the number of steps depending on the time-step size and on the solution) without significant changes in accuracy. However, if they are frozen for too long, there is a loss in precision. In figure (1) we display results obtained with the non-linear method (NLG) (in diagnostic form and with the high modes frozen for every 30 time-steps) and with the pseudo-spectral Galerkin (GL) method at several resolutions. In these tests a small time-step ($\Delta t = 9$ min.) was employed, in order to keep the time truncation errors very small. In this way we can observe better the differences in spatial resolution of both methods. The results, after 200 time steps, show that the non-linear method at a resolution N, has an accuracy close to that of the corresponding Galerkin method at same truncation and considerably better than the acuraccy of the Galerkin method at resolution $N/2$. The lower cost of the non-linear

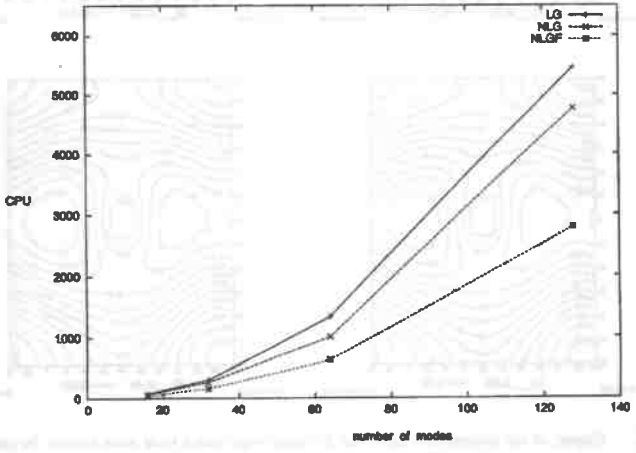

FIG. 2. CPU time

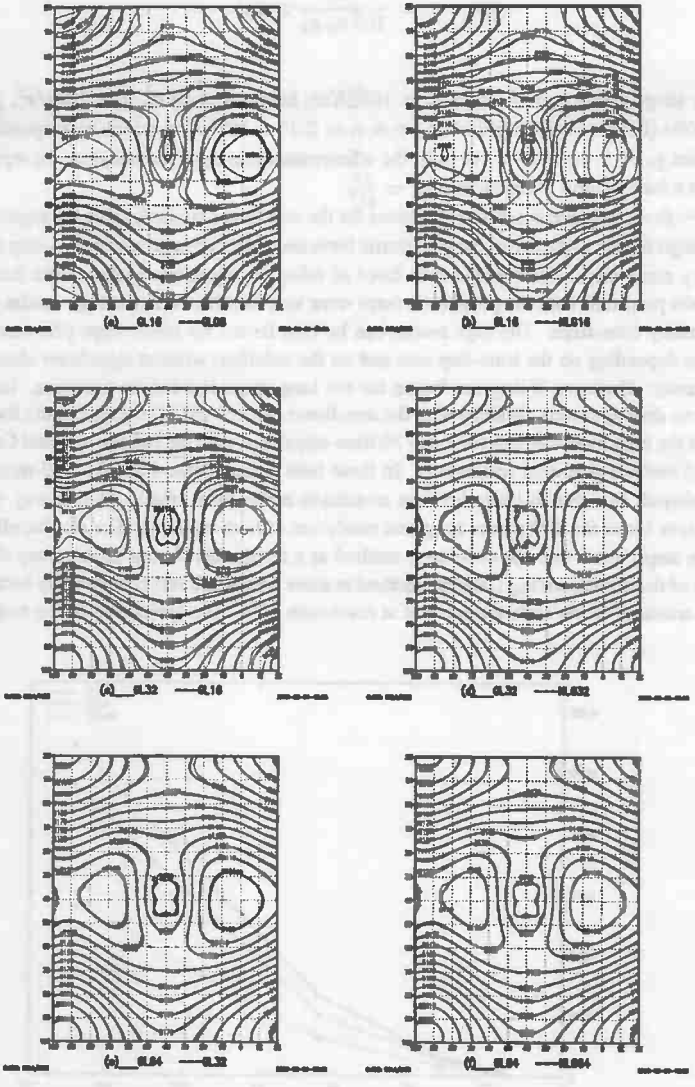

FIG. 3. Display of the geopotential field after 200 time-steps with a local mass source. In the left (plots a, c and e) we compare the results of the (linear) Galerkin method with truncations $N = 16, 32$ and 64 to the results of the same method at half resolution ($N = 8, 16$ and 32) respectively. In the right (plots b,d and f) the Galerkin (LG) method (with truncations $N = 16, 32$ and 64) is compared to the non-linear method (NLG) at same resolution (truncations $N = 16, 32$ and 64, respectively).

Galerkin method (compared to the Galerkin method at same truncation) makes the scheme interesting. In figure (1) the geopotential field is shown for $N = 8, 16$ and 32. In each graphic we compare the linear Galerkin method (GL) at truncation N either to the same method at truncation $N/2$ or to the non-linear method (NLG) at truncation N.

The relative computational efficiency of the schemes can be seen in (2). For N from 16 to 128 we display the CPU times for the whole integration (200 time-steps) with the Linear Galerkin (LG), Non-linear Galerkin (NLG) and Non-linear Galerkin with high modes frozen (NLGF). We observe that the non-linear method (NLG) is faster than LG (for the same resolution) by around 12% and when the high modes are frozen it is almost twice faster.

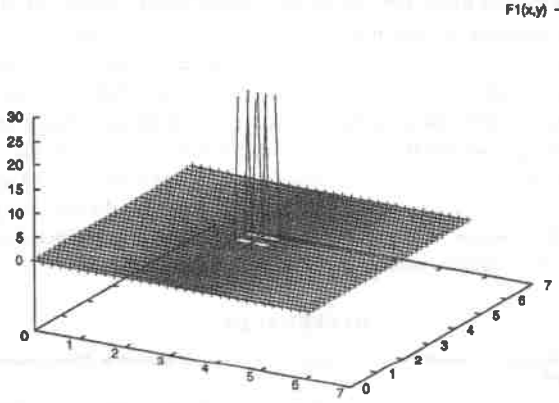

FIG. 4. Shallow Water Equations: Forcing F_1

We also consider less smooth solutions by taking an extra forcing term of the form $F_1(x, y) = \delta_r(x)\delta_r(y)$ where:

$$\delta_r = \begin{cases} \frac{r}{4}(1. + cos(rs + \pi)), & |s| \leq \pi(1 + r) \\ 0, & \text{otherwise} \end{cases}$$

(see Figure (4)). This forcing approximates a local (dirac type) mass source at the center of the domain. The results for the geopotential after 200 time steps (departing from the same initial state as before) are displayed in figure (3). We present results for the linear Galerkin method and for the non-linear method with frozen high modes for every 30 steps, for $N = 8$, 16, 32 and 64. We can observe the same qualitative behaviour of the previous example also in this case, in which at least 32 modes are necessary to provide a good resolution of the solution. Again, the non-linear method at truncation N leads to an intermediate accuracy, between the ones of the Galerkin method at resolutions $N/2$ and N, closer to the latter (at lower cost).

We carried out several stability tests, confirming the CFL-type condition for stability (dependent on the maximal flow velocities). The numerical experiments also confirmed that the non-linear method at truncation N is as stable as the Galerkin method at resolution $N/2$ (being able to employ time steps twice larger than the Galerkin method at truncation N). This is a potential advantage of the non-linear method.

7. CONCLUSIONS

We present a non-linear (pseudo-spectral) Galerkin method for the shallow-water equations on bidimensional periodic domains, and compare it to a pseudo-spectral Galerkin method. Both schemes employ a semi-implicit second-order accurate time discretization, and have a CFL stability restriction governed by the flow velocities, and not by the fast gravity wave modes of the shallow-water equations. This stability condition is more restrictive (by a factor two) for the Galerkin method than for the non-linear scheme. This fact is verified numerically and supported by a linear stability analysis, in which the stability criteria are derived. Both schemes are derived to be free of aliasing due to non linear interaction. With the linear Galerkin method, employing double Fourier expansions with N modes in each direction, this is achieved at the cost of using a $3N/2 \times 3N/2$ auxiliary grid in the spectral transforms. In the non-linear Galerkin method we developed, a $N \times N$ grid is sufficient for alias free computations. In this way, every time step of the non-linear Galerkin method is faster than the corresponding step of the linear Galerkin method at same resolution. In the non-linear method we can also freeze the high-modes for many time-steps, therefore reducing the computational work by a significant amount. Our numerical results indicate that the non-linear Galerkin method, even with the high-modes frozen for many steps, still achieves an accuracy comparable to that of the linear scheme at same resolution, at a considerable lower cost. This fact makes the approach potentially interesting for applications. We are currently investigating its use on spectral schemes for global shallow-water models, with atmospheric applications in view.

REFERENCES

1. Canuto, C., Y. Hussaini, A. Quarteroni, and T. Zang (1988). *Spectral Methods in Fluid Dynamics*, Springer Verlag, New York.

2. Cardenas, J. W. (1999). *Variedades Inerciais Aproximadas e Métodos de Galerkin não linear para as equações de água rasa* (Approximate inertial manifolds and non-linear Galerkin methods for the shallow-water equations), PHd thesis, Universidade de São Paulo, S. Paulo, Brasil.

3. Debussche, A., T. Dubois, and R. Temam (1993). *The nonlinear Galerkin method: A multi-scale method applied to the simulation of homogeneous turbulent flows*, Icase Report No. 93-93.

4. Dettori, L., D. Gottlieb, and R. Temam (1995). *A Nonlinear Galerkin Method: The Two-Level Fourier-Collocation Case*, J. Sci. Comput. 10 (4), 371-389.

5. di Martino, B., and P. Orenga (1998). *Résolution des équations de shallow water par la méthode de Galerkin non linéaire, M^2AN* Math. Model. Numer. Anal. 32, 451-477.

6. Dubois, T., F. Jabertau, and R. Temam (1993). *Solution of the incompressible Navier-Stokes equations by the Nonlinear Galerkin Methods*, J. Sci. Comput. 8 (2), 167-194.

7. Eliasen, E., B. Machenhauer, and E. Rasmussen (1970). *On a numerical method for integration of the hydrodynamical equations with a spectral representation of the horizontal fields*, Report Nr. 2, Institut for Teoretisk Meteorologi, København Universitet, Haraldsgade 6, DK-2200 Copenhagen N, Denmark.

8. Foias, C., O. P. Manley, and R. Temam (1988). *Modelization of the iteration of small and large eddies in two dimensional turbulent flows M^2AN* Math. Model. Numer. Anal. 22, 93-114.

9. Gottlieb, D., and R. Temam (1993). *Implementation of the Nonlinear Galerkin Method with pseudospectral (collocation) discretizations*, Appl. Num. Math. 12, 119-134.

10. Jabertau, F., C. Rosier, and R. Temam (1990). *A Nonlinear Galerkin Method for the Navier-Stokes Equation*, Computer Meth. in Appl. Mechanics and Engineering 80, p.245.

11. Lorenz, E. (1980). *Attractor Sets and Quasi-Geostrophic Equilibrium*, J. Atmos. Sci. 37, 1685-1689.

12. Marion, M., and R. Temam (1989). *Nonlinear Galerkin Methods*, SIAM J. Num. Anal. 26, 1139-1157.

13. Orzag, S. A. (1970). *Transform method for calculation of vector-coupled sums: Application to the spectral form of the vorticity equation*, J. Atmos. Sci. 27, 890-895.

RELATÓRIOS TÉCNICOS DO DEPARTAMENTO DE MATEMÁTICA APLICADA

2000

RT-MAP-0001 – Laércio C. Barros, Suzana A. O. Souza & Pedro Aladar Tonelli
"Two Cases of Asymptotic Smoothness for Fuzzy Dynamical Systems"
February 16, 2000 - São Paulo - IME-USP - 10 pg.

RT-MAP-0002 – Carlos Juiti Watanabe, Paulo Sérgio Pereira da Silva & Pedro Aladar Tonelli
"Álgebra Diferencial em Teoria de Controle"
Abril, 2000 - São Paulo - IME-USP - 14 pg.

RT-MAP-0003 – Eduardo Colli & Edson Vargas
"An Open Set of Initial Conditions Can Draw a Hyperbolic Horseshoe"
April, 3, 2000 - São Paulo - IME-USP - 32 pg.

RT-MAP-0004 – Eduardo Colli
"A Starting Condition Approach to Parameter Distortion in Generalized Renormalization"
Mayl, 4, 2000 - São Paulo - IME-USP - 60 pg.

RT-MAP-0005 – Waldyr Muniz Oliva
"Geometric Mechanics"
June, 2000 - São Paulo - IME-USP - 160 pg.

RT-MAP-0006 - Frank Michael Forger
" Finite Groups for the Genetic Code I: Codon Representations"
August, 2000 - São Paulo - IME-USP

RT-MAP-0007 - Garcia, M.V.P. , Possani, C. , Ranvaud, R. e Tal, F. A.
"THREE THEOREMS ON GRADIENT FIELDS POTENTIALLY USEFUL IN HOMING PIGEON NAVEGATION"
August, 2000 - São Paulo - IME-USP - 14 pg

RT-MAP-0008 – Saulo R. M. Barros, José W. Cárdenas
"A non-linear Galerkin method for the shallow-water equations on periodic domains"
September, 2000 – São Paulo – IME-USP – 16 pg.